European Journal of Medicinal Chemistry 272 (2024) 116478

Contents lists available at ScienceDirect

European Journal of Medicinal Chemistry

journal homepage: www.elsevier.com/locate/ejmech

Research paper

Anticancer activity of 8-hydroxyquinoline-triphenylphosphine rhodium(III) complexes targeting mitophagy pathways

Xiao-Qiong Huang [a,1], Run-Chun Wu [a,1], Jian-Min Liang [a], Zhen Zhou [a,**], Qi-Pin Qin [a,b,*], Hong Liang [b,***]

[a] Guangxi Key Lab of Agricultural Resources Chemistry and Biotechnology, College of Chemistry and Food Science, Yulin Normal University, 1303 Jiaoyudong Road, Yulin 537000, PR China

[b] State Key Laboratory for the Chemistry and Molecular Engineering of Medicinal Resources, School of Chemistry and Pharmacy, Guangxi Normal University, 15 Yucai Road, Guilin, 541004, PR China

ARTICLE INFO

Keywords:
Rh(III) complexes
Triphenylphosphine-8-hydroxyquinolines
Cell apoptosis
ATP
Mitophagy pathways

ABSTRACT

Metallodrugs exhibiting distinct mechanisms of action compared with cisplatin hold promise for overcoming cisplatin resistance and improving the efficacy of anticancer drugs. In this study, a new series of rhodium (Rh) (III) complexes containing tris(triphenylphosphine)rhodium(I) chloride [$(TPP)_3RhCl$] (TPP = triphenylphosphine, TPP=O = triphenylphosphine oxide) and 8-hydroxyquinoline derivatives (H-XR1–H-XR4), namely [$Rh(XR1)_2(TPP)Cl$]·(TPP=O) (Yulin Normal University-1a [**YNU-1a**]), [$Rh(XR2)_2(TPP)Cl$] (**YNU-1b**), [$Rh(XR3)_2(TPP)Cl$] (**YNU-1c**), and [$Rh(XR4)_2(TPP)Cl$] (**YNU-1d**), was synthesized and characterized via X-ray diffraction, mass spectrometry and IR. The cytotoxicity of the compounds **YNU-1a**–**YNU-1d** in Hep-G2 and HCC1806 human cancer cell lines and normal HL-7702 cell line was evaluated. **YNU-1c** exhibited cytotoxicity and selectivity in HCC1806 cells ($IC_{50} = 0.13 \pm 0.06$ μM, selectivity factor (SF) = 384.6). The compounds **YNU-1b** and **YNU-1c**, which were selected for mechanistic studies, induced the activation of apoptotic pathways and mitophagy. In addition, these compounds released cytochrome *c*, cleaved caspase-3/pro-caspase-3 and down-regulated the levels of mitochondrial respiratory chain complexes I/IV (M1 and M4) and ATP. The compound **YNU-1c**, which was selected for in vivo experiments, exhibited tumor growth inhibition (58.9 %). Importantly, hematoxylin and eosin staining and TUNEL revealed that HCC1806 tumor tissues exhibited significant apoptotic characteristics. **YNU-1a**–**YNU-1d** compounds are promising drug candidates that can be used to overcome cisplatin resistance.

1. Introduction

Transition metals have major advantages over organic compounds for the development of new therapeutic drugs, including varying geometries, coordination numbers, oxidation states, and thermodynamic–kinetic characteristics [1–3]. Metal complexes may be used as scaffolds, and a desired therapeutic value can be obtained by incorporating different metal ions and active organic ligands. In vivo, metal ions exist in the form of electron-deficient cations and are readily linked to biological targets of electron-rich biomolecules, such as proteins and DNA, through noncovalent interactions [3,4]. In the 1960s, cisplatin was accidently discovered and demonstrated to possess potent anticancer properties [1,5]. Since then, metal-based chemotherapeutic drugs have gained widespread attention from chemists. Although the rhodium (Rh)(III) center is kinetically inert, a few studies have examined its biological effects [6]. Recent studies have indicated that the incorporation of appropriate ligands increases the reactivity of Rh complexes toward biological targets [6]. These complexes exhibit promising anticancer activity and distinct mechanisms of action (MoAs) compared with platinum drugs. For example, several Rh(III) complexes

* Corresponding author. Guangxi Key Lab of Agricultural Resources Chemistry and Biotechnology, College of Chemistry and Food Science, Yulin Normal University, 1303 Jiaoyudong Road, Yulin 537000, PR China.
** Corresponding author.
*** Corresponding author.
E-mail addresses: zhouzhen0515@126.com (Z. Zhou), qpqin2018@126.com (Q.-P. Qin), hliang@mailbox.gxnu.edu.cn (H. Liang).
[1] These authors contributed equally to this work.

https://doi.org/10.1016/j.ejmech.2024.116478
Received 26 January 2024; Received in revised form 2 May 2024; Accepted 3 May 2024
Available online 4 May 2024

inhibit cell proliferation through various mechanisms, such as mitochondrial dysfunction, autophagy, or immunological pathways [6–13]. Rh-based anticancer complexes can be categorized into two types based on their structure: half-sandwich complexes and cyclometalate complexes [14]. Notably, Guo et al. synthesized a series of organometallic half-sandwich Rh(III) complexes with the structural formula $[(\eta^6\text{-arene})/(\eta^5\text{-Cp*})Rh(XY)Cl]^{0/+}$ (Cp*: $C_5(CH_3)_5$; XY: bidentate chelating ligands), which resulted in cell cycle arrest, disruption of lysosomal integrity [15], and generation of reactive oxygen species (ROS) [12,16].

A survey by Njardarson revealed that nitrogen heterocycles account for 59 % of the small molecule drugs approved by the FDA in 2014 [17], with each drug containing at least one nitrogen heterocycle. The compound 8-hydroxyquinoline (8-OHQ) contains a pyridine ring that provides an N-donor ligand fused with a phenol, which further provides an O-donor ligand; 8-OHQ is the backbone of drugs that form (N, O) five-membered chelate rings with metal ions [18–20]. Derivatives of 8-OHQ exhibit biological activity in several diseases (e.g., 5-nitro-8--OHQ for infectious diseases and 5-chloro-7-iodo-8-OHQ for neuropathies) [18–20]. Recently, many novel quinoline metal complexes, which have shown promising anticancer activity in vitro and in vivo, have been reported, including ruthenium(II) [21–24], copper(II) [25–27], cobalt (II) [25,28], nickel(II) [25,29], zinc(II) [26,30], lanthanide(III) [31], iron(III) [32], platinum(II) [33], vanadium(IV) [34], and Rh(III) [8, 35–38] complexes. Enyedy reported the activity of 8-OHQ–amino acid hybrids and their $[Rh(\eta^5\text{-}C_5Me_5)(H_2O)_3]^{2+}$ complexes, which exhibited high stability and were more effective in treating drug-resistant Colo 320 cells than drug-sensitive Colo 205 cells [35]. Moreover, they interacted with calf thymus DNA (ct-DNA) as well as human serum albumin, but DNA cleavage was not observed [36]. In addition, Chen and Liang synthesized the novel 8-OHQ–Rh complex and found that the unsubstituted and methyl-substituted 8-OHQ–Rh(III) complex can induce tumor cell death by disrupting mitochondrial-related mechanisms [37,38]; however, the specific underlying MoAs remain unknown.

Compounds conjugated to lipophilic cations, such as triphenylphosphine (Ph_3P^+, TPP), can accumulate in the mitochondria driven by plasma membrane potential ($\Delta\psi_p$) and mitochondrial membrane potential ($\Delta\psi_m$) [39–42]. Thus, TPP has been used as a mitochondrial targeting moiety. In this study, we synthesized and characterized four mitochondria-targeting Rh(III) complexes: $[Rh(XR1)_2(TPP)Cl]\cdot(TPP{=}O)$ (**YNU-1a**), $[Rh(XR2)_2(TPP)Cl]$ (**YNU-1b**), $[Rh(XR3)_2(TPP)Cl]$ (**YNU-1c**), and $[Rh(XR4)_2(TPP)Cl]$ (**YNU-1d**), bearing 2-methylquinolin-8-ol (H-XR1), 5,7-dichloro-8-OHQ (H-XR2), 5,7-dichloro-2-methyl-8-OHQ (H-XR3), 2-methyl-5,7-dibromo-quinoline-8-ol (H-XR4), and $(TPP)_3RhCl$. The anti-proliferative activities of these complexes on Hep-G2 and HCC1806 tumor cells and human normal liver HL-7702 cells were evaluated via the MTT assay, and a series of in vitro and in vivo experiments were performed using **YNU-1a**–**YNU-1d** compounds with promising activity.

2. Results and discussion

2.1. Synthesis and stability of YNU-1a–YNU-1d

YNU-1a–**YNU-1d** compounds were synthesized via the reaction of H-XR1–H-XR4 (0.2 mmol) and $(TPP)_3RhCl$ (0.1 mmol; CAS number: 14694-95-2) in mixtures of CH_3OH (1.5 mL) and CH_2Cl_2 (0.1 mL), respectively, and the mixtures were heated at 80 °C for 72 h. The red–brown products of **YNU-1a**–**YNU-1d** eventually appeared, which were isolated and characterized (Scheme 1).

The structure of the novel **YNU-1a**–**YNU-1d** complexes was characterized via X-ray crystallography (Figs. 1–4 and Tables S1–S12), IR (Figs. S1–S4), ESI-MS (Figs. S5–S12) and HNMR (S13–S15). As shown in Figs. 1–4, the Rh(III) center in **YNU-1a**–**YNU-1d** adopted a six-coordinated octahedral geometry. Furthermore, **YNU-1a**–**YNU-1d** compounds were tested for stability in Tris-HCl buffer via ESI-MS (Figs. S5–S12). The main peaks in the mass spectra of **YNU-1a**–**YNU-1d** compounds were detected at 681.35, 791.00, 819.15, and 996.95, respectively, at 0 h, which remained unchanged even after 48 h (Figs. S5–S12), indicating that **YNU-1a**–**YNU-1d** compounds were stable

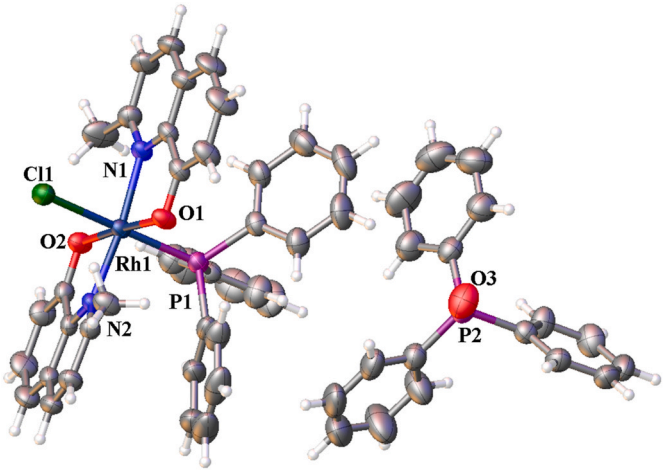

Fig. 1. ORTEP drawing of **YNU-1a**.

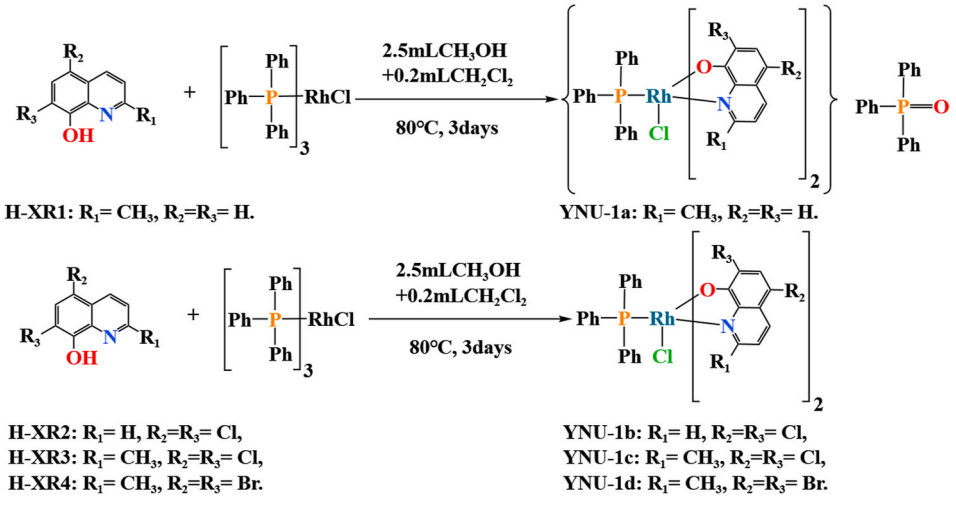

Scheme 1. Synthesis of **YNU-1a**–**YNU-1d** compounds.

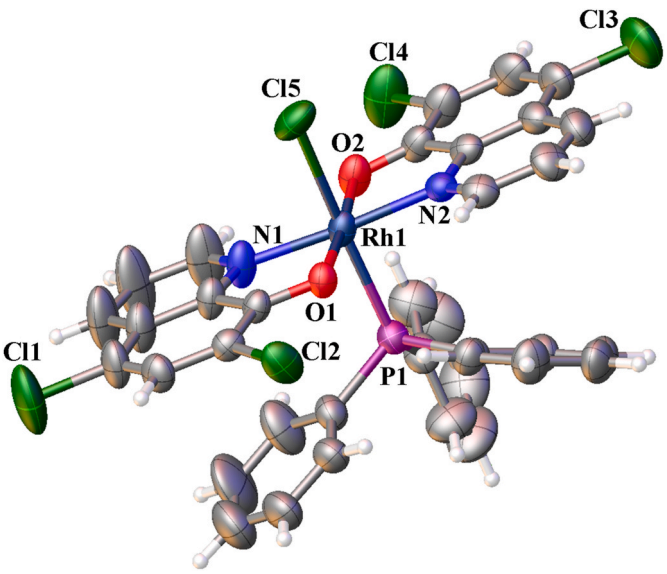

Fig. 2. ORTEP drawing of **YNU-1b**.

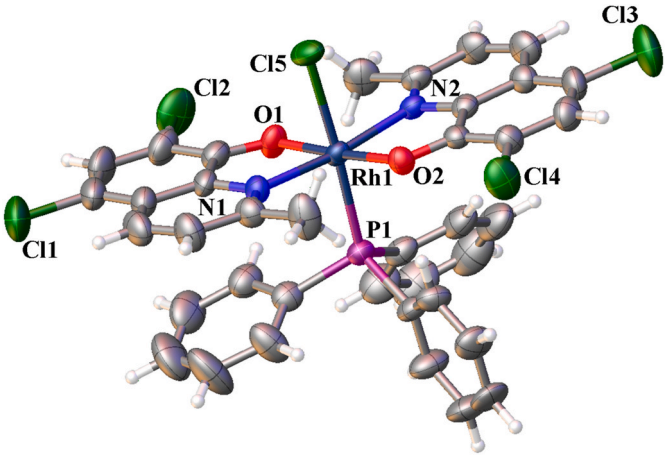

Fig. 3. ORTEP drawing of **YNU-1c**.

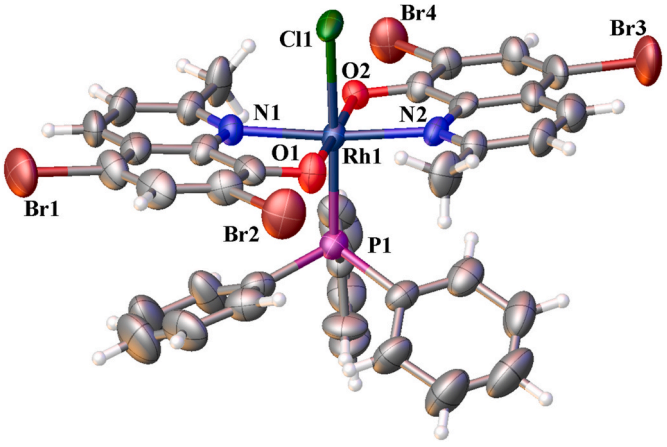

Fig. 4. ORTEP drawing of **YNU-1d**.

in Tris-HCl buffer for 48 h.

2.2. Crystallography

The crystal structures of **YNU-1a**–**YNU-1d** compounds were determined for Rh(III) complexes using the 8-OHQ derivatives H-XR1–H-XR4. The deposition numbers 2327096–2327099 indicate the CCDC numbers for **YNU-1a**–**YNU-1d.** Data regarding the Rh(III) complexes **YNU-1a**–**YNU-1d** are available for free at http://www.ccdc.cam.ac.uk. For these four Rh(III) complexes **YNU-1a**–**YNU-1d** formed via N_2O_2PClRh, Rh(III) demonstrated a slightly distorted six-coordinated octahedral structure surrounded by two 8-OHQ derivative ligands (N^O–Rh), one Cl atom, and one P atom (Figs. 1–4). The lengths of Rh–N, Rh–Cl, and Rh–O bonds (Tables S1–S12), ranging from 2.015(3) to 2.083(8), 2.3951(10) to 2.408(2), and 2.003(3) to 2.0379(19) Å, respectively, were within the normal range.

2.3. In vitro antiproliferative activity

The test compounds **YNU-1a**–**YNU-1d**, parental compounds H-XR1–H-XR4, and cisplatin as a control were evaluated for their antiproliferative activity in Hep-G2 (hepatocellular carcinoma cells), HCC1806 (breast squamous carcinoma cells), and normal liver cell line HL-7702 using the MTT assay [43,44]. The test compounds **YNU-1a**–**YNU-1d** exhibited high antiproliferative activity against the tumor cell lines (IC_{50} = 0.13–3.71 μM), whereas the parental compounds H-XR1–H-XR4 showed low cytotoxicity with an IC_{50} value of >50 μM. In particular, the compound **YNU-1c** showed the highest cytotoxicity against HCC1806 cells with an IC_{50} value of 0.13 ± 0.06 μM (Table 1), which was 69.38-fold higher than that of cisplatin, but it was less toxic to the normal cell line HL-7702 (IC_{50} > 50 μM). The overall trend in the potency of the compounds was as follows: **YNU-1c** > **YNU-1d** > **YNU-1b** > **YNU-1a** > cisplatin ≫ H-XR1–H-XR4. Moreover, for the **YNU-1c**-treated group, the ratio of IC_{50} for HL-7702 to that for HCC1806 (i.e., selectivity factor [6]) was the highest at 384.6, which indicates the selectivity of **YNU-1c** for the tumor cell line HCC1806. The multi-substituted 8-OHQ complexes (**YNU-1b**–**YNU-1d**) exhibited better activity than the single-substituted complex (**YNU-1a**). Furthermore, the addition of a methyl group at 2-position of 8-OHQ increased the potency of the compound **YNU-1c** by 3.6-fold compared with that of compound **YNU-1b** for HCC1806 tumors. The methyl group may contribute to its potency. Importantly, compared with the previously reported Rh complex containing 2-methyl-substituted 8-OHQ ligands [38], **YNU-1c** exhibited a higher potency against Hep-G2 and HCC1806 cells. Moreover, the coordination of TPP to the metal Rh plays a key role [39–42]. For a better comparison and considering the antitumor activity effects of compounds **YNU-1b** and **YNU-1c**, it is reasonable to select these

Table 1
Antiproliferative activity (IC_{50}[a], μM) of **YNU-1a**–**YNU-1d** against HepG2, HCC1806, and HL-7702 cells for 48 h.

	Hep-G2	HCC1806	HL-7702	SF1[b]	SF2[c]
H-XR1	>50	>50	>50	~1.0	1.0
YNU-1a	3.71 ± 0.61	3.01 ± 0.75	>50	>16.6	>13.5
H-XR2	>50	>50	>50	~1.0	~1.0
YNU-1b	0.59 ± 0.22	0.47 ± 0.46	>50	>106.4	>84.7
H-XR3	>50	>50	>50	~1.0	~1.0
YNU-1c	0.19 ± 0.08	0.13 ± 0.06	>50	>384.6	>263.2
H-XR4	>50	>50	>50	~1.0	~1.0
YNU-1d	0.35 ± 0.11	0.31 ± 0.09	>50	>161.3	>142.9
cisplatin	9.89 ± 1.28	9.02 ± 0.49	18.37 ± 1.12	2.0	1.9

[a] IC_{50} values are expressed as the mean ± standard deviation of three independent experiments. Stock solutions of **YNU-1a**–**YNU-1d** (2 mM) were made in DMSO. cisplatin (1.0 mM) was prepared in 0.154 M NaCl. All the experiments contained media with 0.5 % DMSO.

[b] SF1 (selectivity factor 1) = IC_{50} (HL-7702)/IC_{50} (HCC1806).

[c] SF2 (selectivity factor 2) = IC_{50} (HL-7702)/IC_{50} (Hep-G2).

compounds for further biological activity studies.

2.4. Release of cytochrome c and caspase-3 cellular activation

It was previously reported that apoptosis induced by the 2-methyl-8-hydroxyquinoline Rh(III) complex occurred by disrupting mitochondria function [38]. Mitochondrial dysfunction involves the release of cytochrome *c* into the cytoplasm, which subsequently activates the caspase-dependent death pathway, leading to apoptosis [45–50]. Therefore, we measured the expression of cytochrome *c* and cleaved caspase-3 via Western blot analysis to determine whether **YNU-1b** and **YNU-1c** induce apoptosis in HCC1806 cells through the mitochondrial pathway. As expected, **YNU-1c** prominently upregulated the expression of cytochrome *c* and cleaved caspase-3 compared with **YNU-1b** following exposure to HCC1806 cells (Fig. 5). In addition, the ratio of cleaved caspase-3/pro-caspase-3 was increased (Fig. 5). These results suggest that cytochrome *c* initiates the activation of caspase-3. To confirm these observations, the release of cytochrome *c* was examined by immunofluorescence analysis. Fluorescence images were captured by confocal microscopy. HCC1806 cells were treated with **YNU-1c** (0.13 μM) and **YNU-1b** (0.47 μM) for 48 h. The green fluorescent intensity was increased (Fig. 6), which suggests that cytochrome *c* was released and further confirmed that **YNU-1c** and **YNU-1b** induces apoptosis through the mitochondrial pathway. Similarly, the intensity of fluorescence produced by **YNU-1c**-treated cells was significantly higher compared with that of the **YNU-1b**-treated cells.

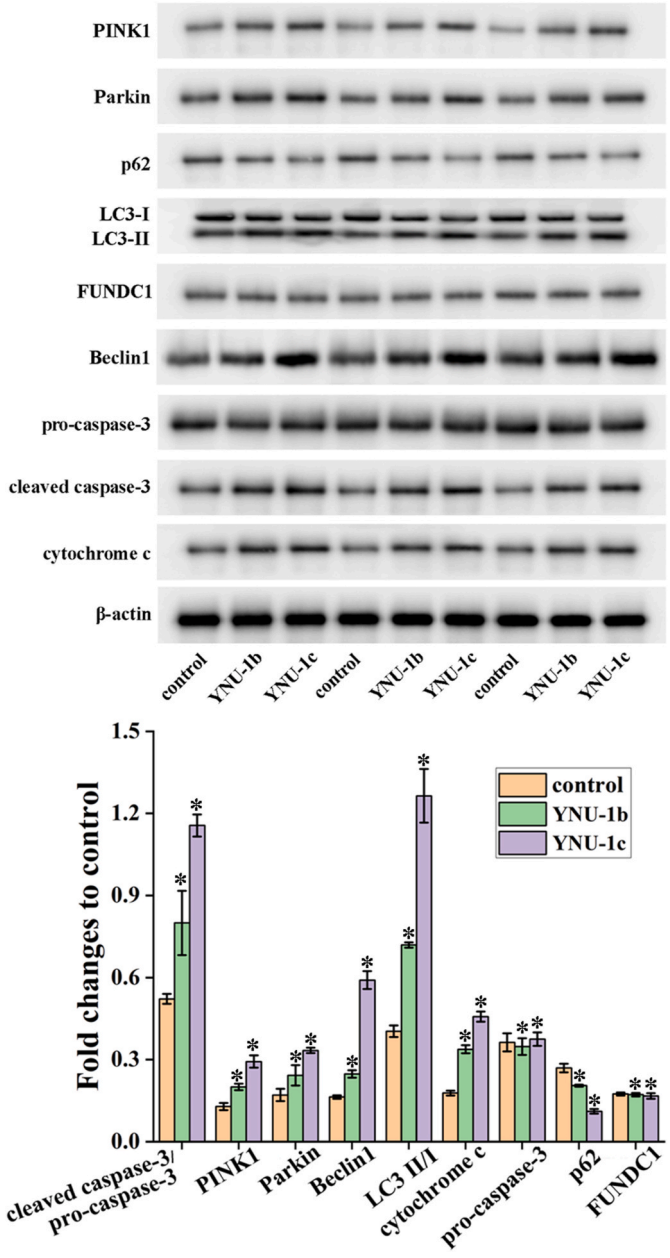

Fig. 5. Levels of mitophagy-related proteins induced by **YNU-1c** (0.13 μM) and **YNU-1b** (0.47 μM) in HCC1806 cells at 48 h, as determined via Western blot analysis. *(*) $p < 0.05$.*

2.5. Mitophagy studies

Autophagy occurs in response to stressful conditions such as hypoxia, starvation, and radiation and acts as a cytoprotective mechanism [51]. In general, autophagy is maintained at a basal level, which contributes to cell survival and homeostasis [51]. A crucial form of autophagy, known as mitophagy, selectively removes damaged mitochondria via the PINK1–Parkin pathway [52]. When mitochondria are depolarized, PINK1 and Parkin accumulate in the mitochondria, ubiquitylate mitochondrial outer membrane proteins, and recruit autophagy-associated proteins, such as p62 and LC3, ultimately leading to mitophagy [53–55]. To determine whether **YNU-1b** and **YNU-1c** promote autophagy, Western blot analysis was used to detect autophagy-related proteins.

The expression levels of PINK1 and Parkin were higher in both **YNU-1b-** and **YNU-1c**-treated groups than in the control group (Fig. 5), indicating that the PINK1–Parkin pathway was activated. The conversion of LC3-I to its lipidation form LC3-II, a specific marker of autophagy, was observed in cells treated with **YNU-1b** and **YNU-1c**. **YNU-1c** showed a higher conversion rate of LC3-I to LC3-II (n = 3) than **YNU-1b**. **YNU-1c** also downregulated the expression of p62, further confirming the autophagic process in HCC1806 cells. In addition, the levels of FUNDC1 protein did not change significantly, but the expression of Beclin-1 was upregulated by **YNU-1c**. These results indicated that **YNU-1b** and **YNU-1c** can induce mitochondrial autophagy, with **YNU-1c** exerting a greater effect. This finding highlights the importance of adding the 2-methyl group to 8-OHQ in **YNU-1c**.

2.6. Mitochondrial respiratory complex activities and ATP energy

As an important organelle involved in cellular metabolism, mitochondria play a vital role in providing the primary source of ATP. The electron transport chain is a series of enzyme complexes that is present within mitochondria. Because some metallic chemotherapeutic agents inhibit M1, M4, and ATP [55–58], we hypothesized that **YNU-1b** and **YNU-1c** may exhibit similar effects. To determine the effect of **YNU-1b** and **YNU-1c** on mitochondrial respiration, the levels of M1, M4, and ATP were measured in HCC1806 cells using M1, M4, and ATP assay kits, respectively.

After 48 h of exposure, the activities of M1 and M4 were decreased in the **YNU-1c**-treated group, with values of 37.38 ± 2.29 U/mg protein and 31.84 ± 1.35 U/mg protein (Table 2 and S13–S15), respectively, which were significantly lower compared with the control sample (66.67 ± 4.00 U/mg protein, 53.18 ± 3.09 U/mg protein) and the **YNU-1b**-treated group (49.03 ± 1.29 U/mg protein, 40.69 ± 0.98 U/mg protein). In addition, the **YNU-1c**-treated group exhibited a decrease in ATP content to 1.77 ± 0.03 μM after 48 h of exposure, which was lower compared with that in the control group (3.51 ± 0.10 μM) and the **YNU-1b**-treated group (2.08 ± 0.10 μM). This decrease in ATP content indicates that **YNU-1b** and **YNU-1c** disrupt mitochondrial function and impede energy production in HCC1806 cells (Table 2 and S13–S15), ultimately leading to cancer cell death. Moreover, it was observed that both **YNU-1b** and **YNU-1c** affected mitochondrial respiration to varying degrees by inhibiting M1, M4, and reducing ATP levels, with **YNU-1c** exhibiting a greater effect.

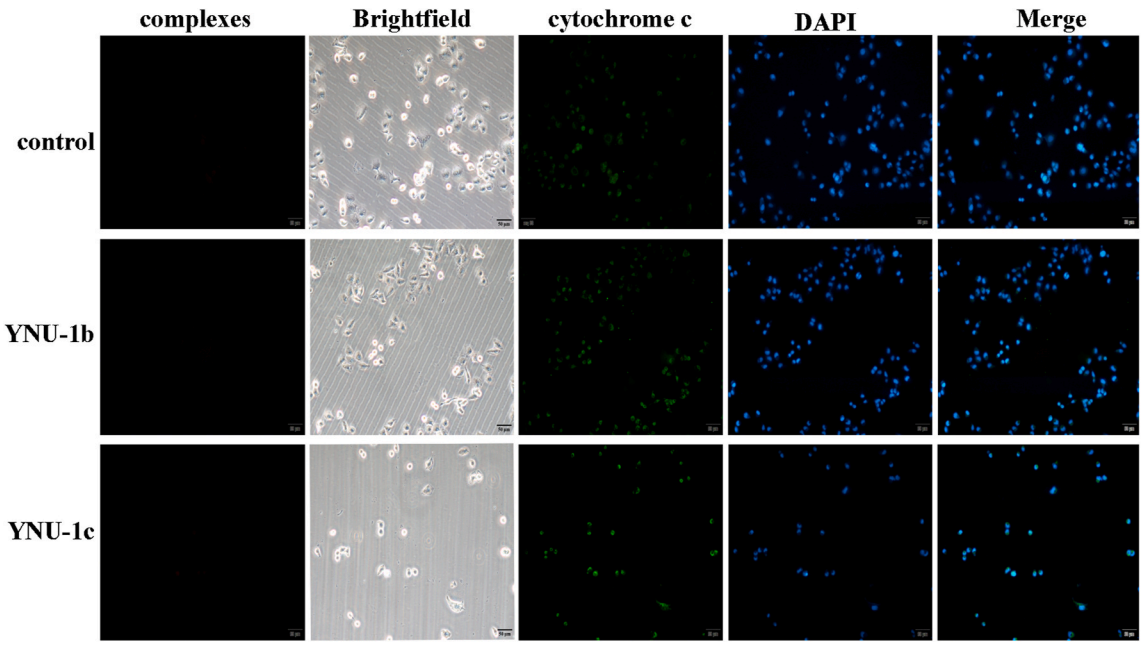

Fig. 6. The release of cytochrome *c* was assessed after exposure of HCC1806 cells to **YNU-1c** (0.13 μM) and **YNU-1b** (0.47 μM) for 48 h via confocal microscopy.

Table 2
Levels of M1, M4, and ATP in HCC1806 cells treated with **YNU-1c** (0.13 μM) and **YNU-1b** (0.47 μM) for 48 h (n = 3, $p < 0.05$).

Group	Complex	Values
M1	Untreated cells	66.67 ± 4.00 U/mg prot
	YNU-1b	49.03 ± 1.29 U/mg prot
	YNU-1c	37.38 ± 2.29 U/mg prot
M4	Untreated cells	53.18 ± 3.09 U/mg prot
	YNU-1b	40.69 ± 0.98 U/mg prot
	YNU-1c	31.84 ± 1.35 U/mg prot
ATP	Untreated cells	3.51 ± 0.10 μM
	YNU-1b	2.08 ± 0.10 μM
	YNU-1c	1.77 ± 0.03 μM

2.7. Apoptosis assay

The MTT assay revealed that **YNU-1b** and **YNU-1c** have a significant effect on the survival of HCC1806 cells. Therefore, apoptosis was assessed by flow cytometry using Annexin V-FITC and PI as indicators of apoptotic and dead cells, respectively [59]. Fig. 7 shows the population of viable cells (FITC−/PI−), early-stage apoptotic cells (FITC+/PI−), and late-stage apoptotic cells (FITC+/PI+) [60] after treatment with **YNU-1c** (0.13 μM) and **YNU-1b** (0.47 μM). HCC1806 cell apoptosis was 28.45 ± 0.88 % for **YNU-1b** and 44.39 ± 1.54 % for **YNU-1c** (Fig. 7). The results indicated that **YNU-1c** was significantly ($p < 0.05$) more effective in promoting HCC1806 cell apoptosis than **YNU-1b**. The results suggest that the observed cytotoxicity of **YNU-1b** and **YNU-1c** in cancer cells primarily occurs through the apoptotic pathway (see Fig. 8).

2.8. In vivo antitumor efficacy

To determine the cytotoxic effect of **YNU-1c** in vivo, HCC1806 tumor-bearing nude mice (Balb/c) were established. These mice were randomly categorized into two groups (n = 6 in each group): control and test groups. **YNU-1c** was intraperitoneally injected at a dose of 5.0 mg/kg every 2 days, and intraperitoneal saline was administered to the control group. In the control group, the growth rate of HCC1806 tumors was extremely high, with the tumor volumes increasing ~16-fold after 21 days. However, the average tumor volume of the **YNU-1c**-treated group increased by only 6.8-fold, revealing that the indicated dose of **YNU-1c** effectively inhibited HCC1806 tumor growth (Tables S16–S18). Furthermore, the tumor weight of the **YNU-1c**-treated group was significantly reduced, resulting in a tumor growth inhibition rate of 58.9 % (Fig. 9). No notable body weight loss was observed in the **YNU-1c**-treated group (Tables S16–S18), suggesting that the mice could tolerate the dose of 5 mg/kg. Taken together, **YNU-1c** may serve as a theranostic platform for inhibiting tumor growth.

2.9. Tumor pathology

The HCC1806 tumor tissues were harvested from the xenograft model for pathological analysis. Hematoxylin and eosin (H&E) staining was done. Hematoxylin causes the nuclear chromatin and cytoplasmic nucleic acids to appear purple–blue, whereas eosin stains the extracellular matrix and cytoplasm red [60,61].

In mice administered **YNU-1c** (5 mg/kg dose), the tumor tissue showed significantly different histological characteristics compared with that of the untreated mice. As shown in Fig. 10, the tumor cells in the control group were uniformly stained without obvious necrotic areas; however, in the **YNU-1c**-treated group, significant cell damage (large pink-stained area) was observed, indicating that **YNU-1c** had visible antitumor effects by inducing apoptosis in vivo. In addition, the TUNEL method was used to identify and quantify apoptotic cells [60,61], which were labeled brown. Fig. 10 shows that the HCC1806 tumor cells exhibited clear characteristics of apoptosis (brown-stained areas), consistent with the results of H&E staining. Statistical analysis revealed that the apoptosis rate of tumors after treatment with **YNU-1c** was 25.11 %, which indicates that **YNU-1c** induces tumor tissue necrosis.

3. Conclusion

We designed and synthesized a series of selective and potent Rh(III) complexes, **YNU-1a–YNU-1d**, featuring H-XR1–H-XR4 and $(TPP)_3RhCl$, and investigated their antiproliferative effects in vitro and in vivo. The MTT assay revealed that **YNU-1b** and **YNU-1c** exerted higher anticancer activity than cisplatin in the tested cancer cells. The methyl group may contribute to its potency. In terms of the underlying mechanism, immunofluorescence analysis, Western blot analysis, and apoptosis assays revealed that **YNU-1b** and **YNU-1c** induce apoptosis in HCC1806

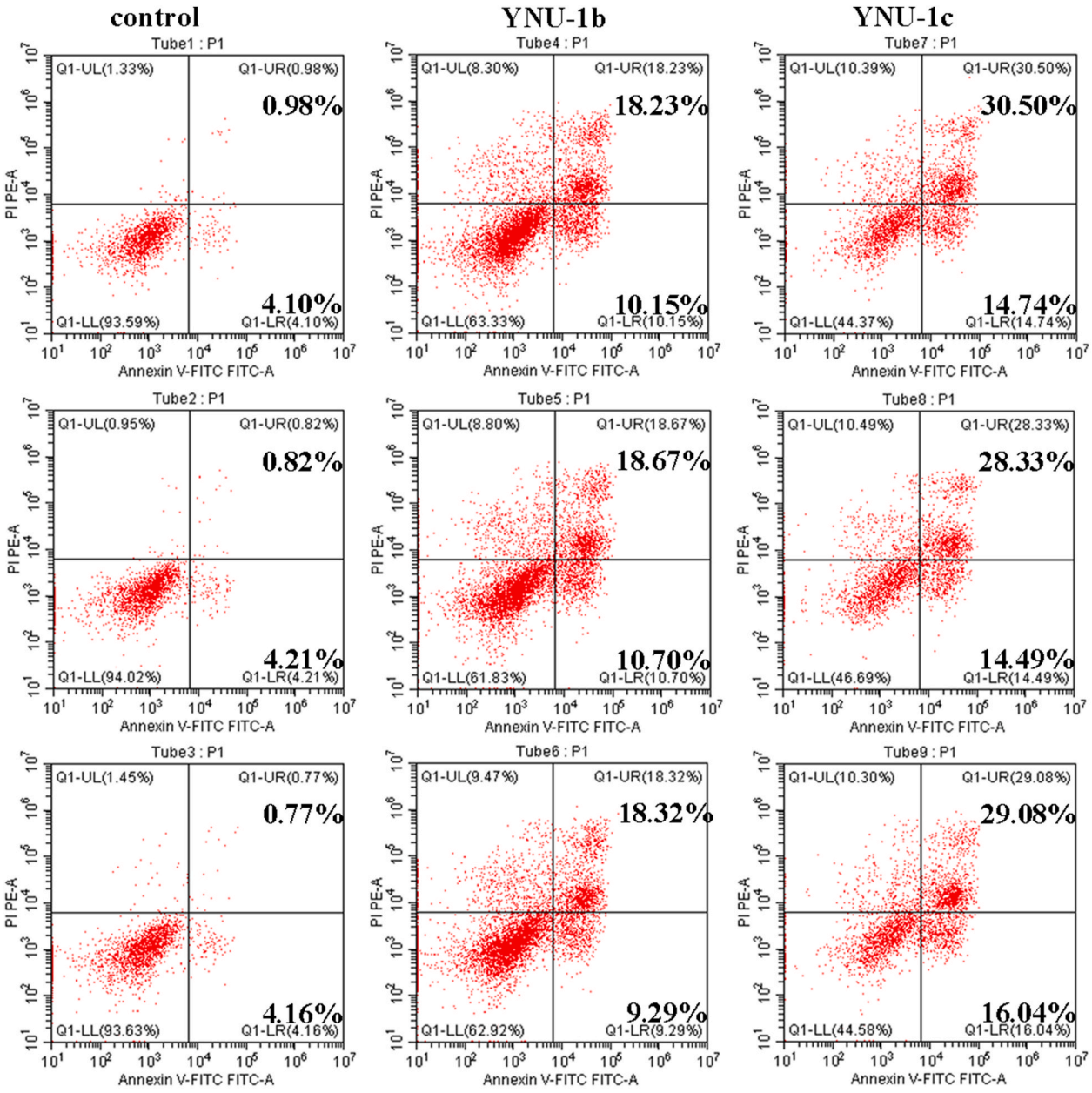

Fig. 7. Apoptosis of HCC1806 cells induced by exposure to **YNU-1c** (0.13 μM) and **YNU-1b** (0.47 μM) for 48 h.

cells. Furthermore, **YNU-1b** and **YNU-1c** induced the release of cytochrome *c* from the mitochondrial intermembrane space into the cytoplasm and further activated caspase-3. Finally, **YNU-1b** and **YNU-1c** induced apoptosis. This indicates the occurrence of mitochondrial dysfunction, and **YNU-1b** exhibited higher potency than **YNU-1c**. Moreover, Western blot analyses revealed that **YNU-1b** and **YNU-1c** activated PINK1–Parkin signaling, inhibited the expression of p62 protein, and further increased the LC3-II/LC3-I ratio and Beclin1, indicating that **YNU-1b** and **YNU-1c** induce mitophagy. In addition, the levels of M1, M4, and ATP were decreased. **YNU-1c** induced apoptosis in a higher proportion of HCC1806 cells in vitro and in vivo than **YNU-1b**. Overall, **YNU-1c** containing a methyl group on its ligand exhibits the strongest antitumor activity and is a potential anticancer metallodrug candidate for treating HCC1806 cells.

4. Experimental methods

4.1. Synthesis of Rh complexes

YNU-1a–**YNU-1d** compounds were synthesized via the reaction of H-L1–H-L4 (0.2 mmol) and $[(C_6H_5)_3P]_3RhCl$ (0.1 mmol) in mixtures of CH_3OH (1.5 mL) and CH_2Cl_2 (0.1 mL), respectively, and the mixtures were heated at 80 °C for 72 h. The red–brown products of **YNU-1a**–**YNU-1d** eventually appeared, which were isolated and characterized (Scheme 1).

Data regarding **YNU-1a**. ESI-MS: m/z = 681.35 for $[M–Cl–(TPP{=}O)]^+$; IR (KBr): 3399, 3053, 1634, 1563, 1505, 1482, 1463, 1434, 1377, 1332, 1283, 1177, 1161, 1113, 1093, 1070, 1038, 997, 885, 831, 751, 722, 693, 641, 581, 542, 531, 513, 498, 482, and 460 cm^{-1}; ^1H NMR (400 MHz, DMSO-d_6): δ 8.01 (d, J = 8.4 Hz, 2H), 7.64–7.59 (m, 20H), 7.55 (m, 10H), 7.28–7.25 (m, 2H), 7.23–7.18 (m, 2H), 7.10–7.05 (m, 2H), 6.79 (m, 2H), 3.10 (s, 6H).

Data regarding **YNU-1b**. ESI-MS: m/z = 791.05 for $[M - Cl]^+$; IR

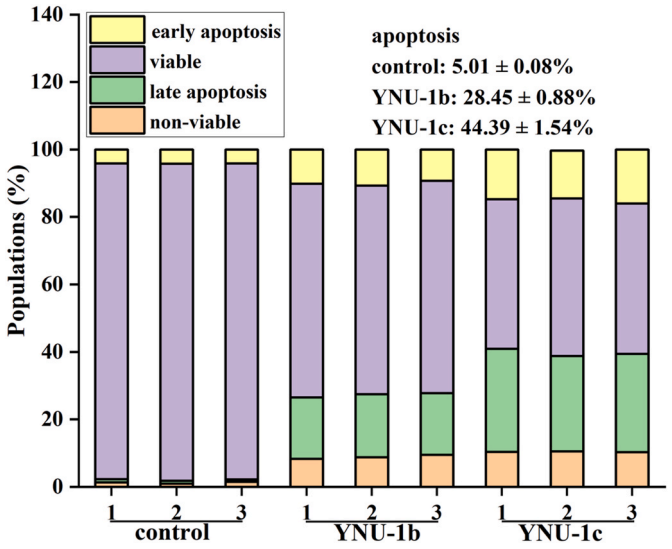

Fig. 8. Populations for the apoptotic HCC1806 cells treated by **YNU-1c** (0.13 μM) and **YNU-1b** (0.47 μM) for 48 h.

(KBr): 3428, 3057, 1962, 1904, 1816, 1620, 1555, 1493, 1483, 1450, 1435, 1399, 1375, 1364, 1289, 1253, 1221, 1195, 1159, 1144, 1118, 1093, 1056, 1028, 998, 978, 887, 848, 812, 777, 749, 694, 660, 619, 547, 519, 499, 463, 440, and 417 cm^{-1}.

Data regarding **YNU-1c**. ESI-MS: m/z = 819.15 for $[M - Cl]^+$; IR (KBr): 3447, 3055, 2987, 2154, 1603, 1582, 1573, 1550, 1499, 1482, 1431, 1368, 1324, 1282, 1266, 1197, 1158, 1121, 1092, 1029, 999, 972, 947, 873, 830, 783, 754, 746, 707, 695, 618, 529, 519, 499, 459, and 438 cm^{-1}; ^1H NMR (400 MHz, DMSO-d_6): δ 8.21 (d, J = 8.6 Hz, 2H), 7.58 (s, 2H), 7.46 (d, J = 8.7 Hz, 2H), 7.33 (td, J = 7.4, 1.8 Hz, 3H), 7.28–7.23 (m, 6H), 7.14 (td, J = 8.2, 2.8 Hz, 6H), 3.24 (s, 6H).

Data regarding **YNU-1d**. ESI-MS: m/z = 996.95 for $[M - Cl]^+$; IR (KBr): 3856, 3819, 3804, 3748, 3673, 3445, 3055, 1572, 1547, 1492, 1482, 1426, 1364, 1321, 1263, 1191, 1151, 1119, 1091, 1028, 999, 952, 936, 870, 829, 760, 746, 695, 675, 529, 514, and 497 cm^{-1}; ^1H NMR (400 MHz, DMSO-d_6): δ 8.14 (d, J = 8.7 Hz, 2H), 7.79 (s, 2H), 7.47 (d, J = 8.7 Hz, 2H), 7.33 (t, J = 7.9 Hz, 3H), 7.28–7.23 (m, 6H), 7.13 (td, J = 8.2, 2.7 Hz, 6H), 3.25 (s, 6H).

4.2. Other experimental methods

The antitumor mechanism of **YNU-1a**–**YNU-1d** in HCC1806 cells was determined as previously described [28,62]. In addition, the detailed data relating to **YNU-1a**–**YNU-1d** and information about experiments can be found in the Electronic Supporting Information Materials.

Abbreviations

SF	selectivity factor
M1	mitochondrial respiratory chain complexes I
M4	mitochondrial respiratory chain complexes IV
ATP	adenosine triphosphate
8-OHQ	8-hydroxyquinoline
$\Delta\psi_p$	plasma membrane potential
Ph_3P^+, TPP	triphenylphosphine
TPP=O	triphenylphosphine oxide
$(TPP)_3RhCl$	tris(triphenylphosphine)rhodium(I) chloride
$\Delta\psi_m$	mitochondrial membrane potential
H-XR1	2-methylquinolin-8-ol
H-XR2	5,7-dichloro-8-OHQ
H-XR3	5,7-dichloro-2-methyl-8-OHQ
H-XR4	2-methyl-5,7-dibromo-quinoline-8-ol
Hep-G2	hepatocellular carcinoma cells
HCC1806	breast squamous carcinoma cells
HL-7702	normal liver cell line
MTT	3-(4,5-Dimethylthiazol-2-yl)-2,5-diphenyltetrazolium bromide
SF1	selectivity factor 1
SF2	selectivity factor 2
H&E	hematoxylin and eosin (H&E) staining
MoAs	mechanisms of action
ROS	reactive oxygen species

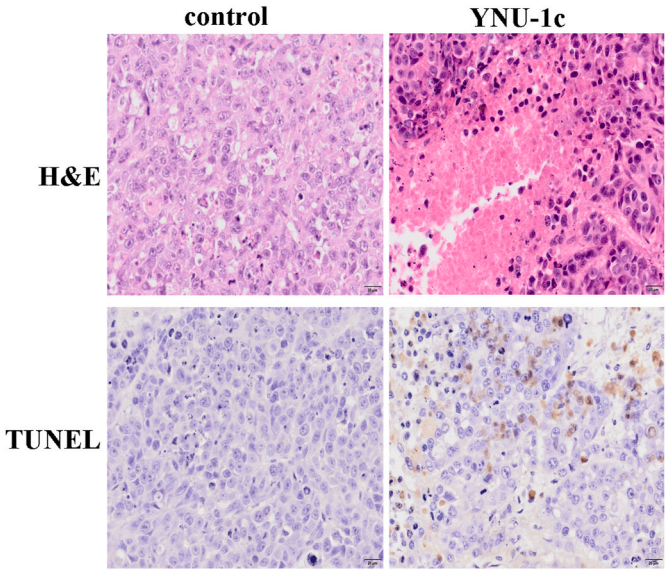

Fig. 10. Effect of **YNU-1c** on tumor tissue compared with the control group.

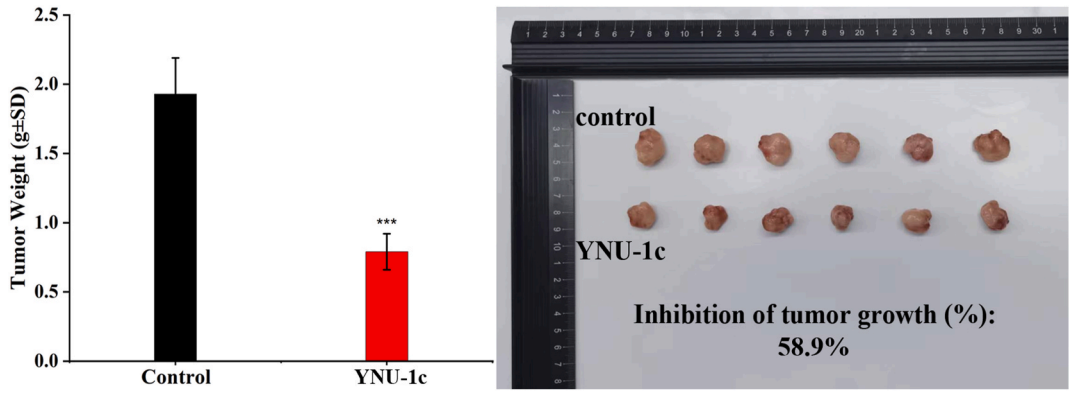

Fig. 9. **YNU-1c** (5.0 mg/kg/q2d) exhibits antitumor effects in an in vivo HCC1806 mouse model.***$p < 0.05$.

CRediT authorship contribution statement

Xiao-Qiong Huang: Validation, Methodology, Data curation, Conceptualization. **Run-Chun Wu:** Validation, Methodology, Formal analysis, Data curation. **Jian-Min Liang:** Formal analysis, Data curation. **Zhen Zhou:** Writing – original draft, Resources, Funding acquisition. **Qi-Pin Qin:** Writing – review & editing, Writing – original draft, Supervision, Formal analysis, Data curation, Conceptualization. **Hong Liang:** Supervision, Resources, Project administration, Formal analysis.

Declaration of competing interest

The authors declare that they have no known competing financial interests or personal relationships that could have appeared to influence the work reported in this paper.

Data availability

The data presented in this study are available upon request from the corresponding author. The data are not publicly available because of project confidentiality.

Acknowledgments

We thank the National Natural Science Foundation of China (China, Grant No. 22267020), Natural Science Foundation of Guangxi (Grant No. 2020GXNSFAA297077), and Talent Project of Yulin Normal University (China, Grant Nos. G2023ZK05, G2023ZK19, G2022ZK24, and G2022ZK25).

Appendix A. Supplementary data

Supplementary data to this article can be found online at https://doi.org/10.1016/j.ejmech.2024.116478.

References

[1] S.H. van Rijt, P.J. Sadler, Current applications and future potential for bioinorganic chemistry in the development of anticancer drugs, Drug Discov. Today 14 (2009) 1089–1097.
[2] M. Sohrabi, M. Saeedi, B. Larijani, M. Mahdavi, Recent advances in biological activities of rhodium complexes: their applications in drug discovery research, Eur. J. Med. Chem. 216 (2021) 113308.
[3] U. Das, B. Kar, S. Pete, P. Paira, Ru(II), Ir(III), Re(I) and Rh(III) based complexes as next generation anticancer metallopharmaceuticals, Dalton Trans. 50 (2021) 11259–11290.
[4] T. Storr, K.H. Thompson, C. Orvig, Design of targeting ligands in medicinal inorganic chemistry, Chem. Soc. Rev. 35 (2006) 534–544.
[5] B. Rosenberg, L. Van Camp, T. Krigas, Inhibition of cell division in escherichia coli by electrolysis products from a platinum electrode, Nature 205 (1965) 698–699.
[6] Y.-Q. Gu, K. Yang, Q.-Y. Yang, H.-Q. Li, M.-Q. Hu, M.-X. Ma, N.-F. Chen, Y.-H. Liu, H. Liang, Z.-F. Chen, Rhodium(III)-picolinamide complexes act as anticancer and antimetastasis agents via inducing apoptosis and autophagy, J. Med. Chem. 66 (2023) 9592–9606.
[7] T.-M. Khan, N.S. Gul, X. Lu, R. Kumar, M.I. Choudhary, H. Liang, Z.-F. Chen, Rhodium(iii) complexes with isoquinoline derivatives as potential anticancer agents: in vitro and in vivo activity studies, Dalton Trans. 48 (2019) 11469–11479.
[8] Z.-F. Wang, X.-L. Nai, Y. Xu, F.-H. Pan, F.-S. Tang, Q.-P. Qin, L. Yang, S.-H. Zhang, Cell nucleus localization and high anticancer activity of quinoline-benzopyran rhodium(III) metal complexes as therapeutic and fluorescence imaging agents, Dalton Trans. 51 (2022) 12866–12875.
[9] Y.-B. Peng, W. He, Q. Niu, C. Tao, X.-L. Zhong, C.-P. Tan, P. Zhao, Mitochondria-targeted cyclometalated rhodium(III) complexes: synthesis, characterization and anticancer research, Dalton Trans. 50 (2021) 9068–9075.
[10] Y.-B. Peng, C. Tao, C.-P. Tan, P. Zhao, Mitochondrial targeted rhodium(III) complexes: synthesis, characterized and antitumor mechanism investigation, J. Inorg. Biochem. 218 (2021) 111400.
[11] C. Pérez-Arnaiz, M.I. Acuña, N. Busto, I. Echevarría, M. Martínez-Alonso, G. Espino, B. García, F. Domínguez, Thiabendazole-based Rh(III) and Ir(III) biscyclometallated complexes with mitochondria-targeted anticancer activity and metal-sensitive photodynamic activity, Eur. J. Med. Chem. 157 (2018) 279–293.
[12] L. Guo, P. Li, J. Li, Y. Gong, X. Li, Y. Liu, K. Yu, Z. Liu, Half-sandwich iridium(III), rhodium(III), and ruthenium(II) complexes chelating hybrid sp^2-N/sp^3-N donor ligands to achieve improved anticancer selectivity, Inorg. Chem. 62 (2023) 15118–15137.
[13] Y. Zheng, X.-X. Chen, D.-Y. Zhang, W.-J. Wang, K. Peng, Z.-Y. Li, Z.-W. Mao, C.-P. Tan, Activation of the cGAS-STING pathway by a mitochondrial DNA-targeted emissive rhodium(III) metallointercalator, Chem. Sci. 14 (2023) 6890–6903.
[14] X. Hu, L. Guo, M. Liu, Q. Zhang, Y. Gong, M. Sun, S. Feng, Y. Xu, Y. Liu, Z. Liu, Increasing anticancer activity with phosphine ligation in zwitterionic half-sandwich iridium(III), rhodium(III), and ruthenium(II) complexes, Inorg. Chem. 61 (2022) 20008–20025.
[15] L. Guo, X. Hu, Y. Yang, W. An, J. Gao, Q. Liu, Z. Liu, Synthesis and biological evaluation of zwitterionic half-sandwich rhodium(III) and ruthenium(II) organometallic complexes, Bioorg. Chem. 116 (2021) 105311.
[16] X. Hu, L. Guo, M. Liu, M. Sun, Q. Zhang, H. Peng, F. Zhang, Z. Liu, Formation of iridium(III) and rhodium(III) amine, imine, and amido complexes based on pyridine-amine ligands: structural diversity arising from reaction conditions, substituent variation, and metal centers, Inorg. Chem. 61 (2022) 10051–10065.
[17] E. Vitaku, D.T. Smith, J.T. Njardarson, Analysis of the structural diversity, substitution patterns, and frequency of nitrogen heterocycles among U.S. FDA approved pharmaceuticals, J. Med. Chem. 57 (2014) 10257–10274.
[18] V.F.S. Pape, R. Palkó, S. Tóth, M.J. Szabó, J. Sessler, G. Dormán, É.A. Enyedy, T. Soós, I. Szatmári, G. Szakács, Structure-activity relationships of 8-hydroxyquinoline-derived mannich bases with tertiary amines targeting multidrug-resistant cancer, J. Med. Chem. 65 (2022) 7729–7745.
[19] X. Zhou, Insights of metal 8-hydroxylquinolinol complexes as the potential anticancer drugs, J. Inorg. Biochem. 238 (2023) 112051.
[20] R. Gupta, V. Luxami, K. Paul, Insights of 8-hydroxyquinolines: a novel target in medicinal chemistry, Bioorg. Chem. 108 (2021) 104633.
[21] M. Huang, Y. Zhang, Y. Gong, Z. Liang, X. Chen, Y. Ni, X. Pan, W. Wu, J. Chen, Z. Huang, J. Sun, 8-Hydroxyquinoline ruthenium(II) complexes induce ferroptosis in HeLa cells by down-regulating GPX4 and ferritin, J. Inorg. Biochem. 248 (2023) 112365.
[22] X. Ma, J. Lu, P. Yang, Z. Zhang, B. Huang, R. Li, R. Ye, 8-Hydroxyquinoline-modified ruthenium(II) polypyridyl complexes for JMJD inhibition and photodynamic antitumor therapy, Dalton Trans. 51 (2022) 13902–13909.
[23] X. He, J. Chen, L. Wei, M. Kandawa-Shultz, G. Shao, Y. Wang, Antitumor activity of iridium/ruthenium complexes containing Nitro -substituted quinoline ligands in vivo and in vitro, Dyes Pigments 213 (2023) 111146.
[24] P.K. Anuja, N. Roy, U. Das, S. Varddhan, S.K. Sahoo, P. Paira, [Ru(η^6-*p*-cymene)(N^O 8-hydroxyquinoline)(PTA)] complexes as rising stars in medicinal chemistry: synthesis, properties, biomolecular interactions, in vitro anti-tumor activity toward human brain carcinomas, and in vivo biodistribution and toxicity in a zebrafish model, Dalton Trans. 51 (2022) 8497–8509.
[25] A. Kotian, V. Kamat, K. Naik, D.G. Kokare, K. Kumara, K.L. Neratur, V. Kumbar, K. Bhat, V.K. Revankar, 8-Hydroxyquinoline derived p-halo N4-phenyl substituted thiosemicarbazones: crystal structures, spectral characterization and in vitro cytotoxic studies of their Co(III), Ni(II) and Cu(II) complexes, Bioorg. Chem. 112 (2021) 104962.
[26] L. Côrte-Real, V. Pósa, M. Martins, R. Colucas, N.V. May, X. Fontrodona, I. Romero, F. Mendes, C. Pinto Reis, M.M. Gaspar, J.C. Pessoa, É.A. Enyedy, I. Correia, Cu(II) and Zn(II) complexes of new 8-hydroxyquinoline schiff bases: investigating their structure, solution speciation, and anticancer potential, Inorg. Chem. 62 (2023) 11466–11486.
[27] A. Ali, S. Mishra, S. Kamaal, A. Alarifi, M. Afzal, K.D. Saha, M. Ahmad, Evaluation of catacholase mimicking activity and apoptosis in human colorectal carcinoma cell line by activating mitochondrial pathway of copper(II) complex coupled with 2-(quinolin-8-yloxy)(methyl)benzonitrile and 8-hydroxyquinoline, Bioorg. Chem. 106 (2021) 104479.
[28] Y.-F. Wang, J.-X. Tang, Z.-Y. Mo, J. Li, F.-P. Liang, H.-H. Zou, The strong in vitro and vivo cytotoxicity of three new cobalt(II) complexes with 8-methoxyquinoline, Dalton Trans. 51 (2022) 8840–8847.
[29] Z.-F. Wang, Q.-C. Wei, J.-X. Li, Z. Zhou, S.-H. Zhang, A new class of nickel(II) oxyquinoline-bipyridine complexes as potent anticancer agents induces apoptosis and autophagy in A549/DDP tumor cells through mitophagy pathways, Dalton Trans. 51 (2022) 7154–7163.
[30] L.-Q. Du, T.-Y. Zhang, X.-M. Huang, Y. Xu, M.-X. Tan, Y. Huang, Y. Chen, Q.-P. Qin, Synthesis and anticancer mechanisms of zinc(II)-8-hydroxyquinoline complexes with 1,10-phenanthroline ancillary ligands, Dalton Trans. 52 (2023) 4737–4751.
[31] Y. Yang, Z. Zhou, Z.-Z. Wei, Q.-P. Qin, L. Yang, H. Liang, High anticancer activity and apoptosis- and autophagy-inducing properties of novel lanthanide(III) complexes bearing 8-hydroxyquinoline-N-oxide and 1,10-phenanthroline, Dalton Trans. 50 (2021) 5828–5834.
[32] V. Ferretti, C.P. Matos, C. Canelas, J.C. Pessoa, A.I. Tomaz, R. Starosta, I. Correia, I. E. León, New ternary Fe(III)-8-hydroxyquinoline-reduced Schiff base complexes as selective anticancer drug candidates, J. Inorg. Biochem. 236 (2022) 111961.
[33] Y. Yang, L.-Q. Du, Y. Huang, C.-J. Liang, Q.-P. Qin, H. Liang, Platinum(II) 5-substituted-8-hydroxyquinoline coordination compounds induces mitophagy-mediated apoptosis in A549/DDP cancer cells, J. Inorg. Biochem. 241 (2023) 112152.
[34] N. Ribeiro, I. Bulut, V. Pósa, B. Sergi, G. Sciortino, J.C. Pessoa, L.B. Maia, V. Ugone, E. Garribba, É.A. Enyedy, C. Acilan, I. Correia, Solution chemical properties and anticancer potential of 8-hydroxyquinoline hydrazones and their oxidovanadium (IV) complexes, J. Inorg. Biochem. 235 (2022) 111932.
[35] J.P. Mészáros, J.M. Poljarević, I. Szatmári, O. Csuvik, F. Fülöp, N. Szoboszlai, G. Spengler, É.A. Enyedy, An 8-hydroxyquinoline–proline hybrid with multidrug resistance reversal activity and the solution chemistry of its half-sandwich organometallic Ru and Rh complexes, Dalton Trans. 49 (2020) 7977–7992.
[36] T. Pivarcsik, O. Dömötör, J.P. Mészáros, N.V. May, G. Spengler, O. Csuvik, I. Szatmári, É.A. Enyedy, 8-Hydroxyquinoline-Amino acid hybrids and their half-

sandwich Rh and Ru complexes: synthesis, anticancer activities, solution chemistry and interaction with biomolecules, Int. J. Mol. Sci. 22 (2021) 11281.
[37] H.-R. Zhang, Y.-C. Liu, Z.-F. Chen, T. Meng, B.-Q. Zou, Y.-N. Liu, H. Liang, Studies on the structures, cytotoxicity and apoptosis mechanism of 8-hydroxylquinoline rhodium(III) complexes in T-24 cells, New J. Chem. 40 (2016) 6005–6014.
[38] Y.-L. Zhang, Q.-P. Qin, Q.-q. Cao, H.-H. Han, Z.-L. Liu, Y.-C. Liu, H. Liang, Z.-F. Chen, Synthesis, crystal structure, cytotoxicity and action mechanism of a Rh(iii) complex with 8-hydroxy-2-methylquinoline as a ligand, Med. Chem. Comm 8 (2017) 184–190.
[39] K. Wang, C. Zhu, Y. He, Z. Zhang, W. Zhou, N. Muhammad, Y. Guo, X. Wang, Z. Guo, Restraining cancer cells by dual metabolic inhibition with a mitochondrion-targeted platinum(II) complex, Angew. Chem. Int. Ed. 58 (2019) 4638–4643.
[40] S.E. Weinberg, N.S. Chandel, Targeting mitochondria metabolism for cancer therapy, Nat. Chem. Biol. 11 (2015) 9–15.
[41] W. Zhou, X. Wang, M. Hu, C. Zhu, Z. Guo, A mitochondrion-targeting copper complex exhibits potent cytotoxicity against cisplatin-resistant tumor cells through multiple mechanisms of action, Chem. Sci. 5 (2014) 2761–2770.
[42] Z. Zhu, Z. Wang, C. Zhang, Y. Wang, H. Zhang, Z. Gan, Z. Guo, X. Wang, Mitochondrion-targeted platinum complexes suppressing lung cancer through multiple pathways involving energy metabolism, Chem. Sci. 10 (2019) 3089–3095.
[43] S. Kuang, F. Wei, J. Karges, L. Ke, K. Xiong, X. Liao, G. Gasser, L. Ji, H. Chao, Photodecaging of a mitochondria-localized iridium(III) endoperoxide complex for two-photon photoactivated therapy under hypoxia, J. Am. Chem. Soc. 144 (2022) 4091–4101.
[44] T. Mosmann, Rapid colorimetric assay for cellular growth and survival: application to proliferation and cytotoxicity assays, J. Immunol. Methods 65 (1983) 55–63.
[45] P. Li, D. Nijhawan, I. Budihardjo, S.M. Srinivasula, M. Ahmad, E.S. Alnemri, X. Wang, Cytochrome c and dATP-dependent formation of Apaf-1/Caspase-9 complex initiates an apoptotic protease cascade, Cell 91 (1997) 479–489.
[46] S. Jin, Y. Hao, Z. Zhu, N. Muhammad, Z. Zhang, K. Wang, Y. Guo, Z. Guo, X. Wang, Impact of mitochondrion-targeting group on the reactivity and cytostatic pathway of platinum(IV) complexes, Inorg. Chem. 57 (2018) 11135–11145.
[47] Q.-Y. Liu, Y.-Y. Qi, D.-H. Cai, Y.-J. Liu, L. He, X.-Y. Le, Sparfloxacin- Cu(II)-aromatic heterocyclic complexes: synthesis, characterization and in vitro anticancer evaluation, Dalton Trans. 51 (2022) 9878–9887.
[48] W.-Y. Zhang, F. Du, M. He, L. Bai, Y.-Y. Gu, L.-L. Yang, Y.-J. Liu, Studies of anticancer activity in vitro and in vivo of iridium(III) polypyridyl complexes-loaded liposomes as drug delivery system, Eur. J. Med. Chem. 178 (2019) 390–400.
[49] W.-Y. Zhang, Y.-J. Wang, F. Du, M. He, Y.-Y. Gu, L. Bai, L.-L. Yang, Y.-J. Liu, Evaluation of anticancer effect in vitro and in vivo of iridium(III) complexes on gastric carcinoma SGC-7901 cells, Eur. J. Med. Chem. 178 (2019) 401–416.
[50] Y. Guo, S. Jin, D. Song, T. Yang, J. Hu, X. Hu, Q. Han, J. Zhao, Z. Guo, X. Wang, Amlexanox-modified platinum(IV) complex triggers apoptotic and autophagic bimodal death of cancer cells, Eur. J. Med. Chem. 242 (2022) 114691.
[51] Y. Huang, X. You, L. Wang, G. Zhang, S. Gui, Y. Jin, R. Zhao, D. Zhang, Pyridinium-substituted tetraphenylethylenes functionalized with alkyl chains as autophagy modulators for cancer therapy, Angew. Chem. Int. Ed. 59 (2020) 10042–10051.
[52] M.-M. Wang, F.-J. Xu, Y. Su, Y. Geng, X.-T. Qian, X.-L. Xue, Y.-Q. Kong, Z.-H. Yu, H.-K. Liu, Z. Su, A new strategy to fight metallodrug resistance: mitochondria-relevant treatment through mitophagy to inhibit metabolic adaptations of cancer cells, Angew. Chem. Int. Ed. 61 (2022) e202203843.
[53] (a) M.E. Gegg, A.H.V. Schapira, PINK1-parkin-dependent mitophagy involves ubiquitination of mitofusins 1 and 2: Implications for Parkinson disease pathogenesis, Autophagy 7 (2011) 243–245;
(b) Y. Guo, S. Jin, H. Yuan, T. Yang, K. Wang, Z. Guo, X. Wang, DNA-unresponsive platinum(II) complex induces ERS-mediated mitophagy in cancer cells, J. Med. Chem. 65 (2022) 520–530.
[54] K. Palikaras, E. Lionaki, N. Tavernarakis, Mechanisms of mitophagy in cellular homeostasis, physiology and pathology, Nat. Cell Biol. 20 (2018) 1013–1022.
[55] M. Yu, J. Yang, X. Gao, W. Sun, S. Liu, Y. Han, X. Lu, C. Jin, S. Wu, Y. Cai, Lanthanum chloride impairs spatial learning and memory by inducing $[Ca^{2+}]_m$ overload, mitochondrial fission-fusion disorder and excessive mitophagy in hippocampal nerve cells of rats, Metallomics 12 (2020) 592–606.
[56] Z.-F. Wang, X.-Q. Huang, R.-C. Wu, Y. Xiao, S.-H. Zhang, Antitumor studies evaluation of triphenylphosphine ruthenium complexes with 5,7-dihalo-substituted-8-quinolinoline targeting mitophagy pathways, J. Inorg. Biochem. 248 (2023) 112361.
[57] Z.-F. Wang, X.-F. Zhou, Q.-C. Wei, Q.-P. Qin, J.-X. Li, M.-X. Tan, S.-H. Zhang, Novel bifluorescent Zn(II)-cryptolepine-cyclen complexes trigger apoptosis induced by nuclear and mitochondrial DNA damage in cisplatin-resistant lung tumor cells, Eur. J. Med. Chem. 238 (2022) 114418.
[58] S.-H. Zhang, Z.-F. Wang, H. Tan, Novel zinc(II)-curcumin molecular probes bearing berberine and jatrorrhizine derivatives as potential mitochondria-targeting anti-neoplastic drugs, Eur. J. Med. Chem. 243 (2022) 114736.
[59] W. Lv, Z. Zhang, K.Y. Zhang, H. Yang, S. Liu, A. Xu, S. Guo, Q. Zhao, W. Huang, A mitochondria-targeted Photosensitizer showing improved photodynamic therapy effects under hypoxia, Angew. Chem. Int. Ed. 55 (2016) 9947–9951.
[60] Z. Lv, L. Zou, H. Wei, S. Liu, W. Huang, Q. Zhao, Phosphorescent Starburst Pt(II) Porphyrins as Bifunctional therapeutic agents for tumor hypoxia imaging and photodynamic therapy, ACS Appl. Mater. Interfaces 10 (2018) 19523–19533.
[61] J. Qi, Y. Zheng, B. Li, L. Wei, J. Li, X. Xu, S. Zhao, X. Zheng, Y. Wang, Mechanism of vitamin B6 benzoyl hydrazone platinum(II) complexes overcomes multidrug resistance in lung cancer, Eur. J. Med. Chem. 237 (2022) 114415.
[62] (a) C.-J. Liang, R.-C. Wu, X.-Q. Huang, Q.-P. Qin, H. Liang, M.-X. Tan, Synthesis and anticancer mechanisms of four novel platinum(II) 4′-substituted-2,2′:6′,2″-terpyridine complexes, Dalton Trans. 53 (2024) 2143–2152;
(b) L.-Q. Du, C.-J. Zeng, D.-Y. Mo, Q.-P. Qin, M.-X. Tan, H. Liang, 8-hydroxyquinoline-N-oxide copper(II)- and zinc(II)-phenanthroline and bipyridine coordination compounds: Design, synthesis, structures, and antitumor evaluation, J. Inorg. Biochem. 251 (2024) 112443;
(c) Z.-F. Chen, Q.-P. Qin, J.-L. Qin, Y.-C. Liu, K.-B. Huang, Y.-L. Li, T. Meng, G.-H. Zhang, Y. Peng, X.-J. Luo, H. Liang, Stabilization of G-Quadruplex DNA, Inhibition of telomerase activity, and tumor cell apoptosis by organoplatinum(II) complexes with oxoisoaporphine, J. Med. Chem. 58 (2015) 2159–2179;
(d) Q.-P. Qin, Z.-Z. Wei, Z.-F. Wang, X.-L. Huang, M.-X. Tan, H.-H. Zou, H. Liang, Imaging and therapeutic applications of Zn(II)-cryptolepine–curcumin molecular probes in cell apoptosis detection and photodynamic therapy, Chem. Commun. 56 (2020) 3999–4002.